A Multiphase Pump Unit for the Offshore Exploitation of Oil-Gas-Solid Mixtures

*By TH. HERPEL, S. MUSCHELKNAUTZ and F. MAYINGER**

Abstract

The further exploration of crude oil offshore will lead to the exploitation of smaller oil reservoirs, which are located around the nowadays discovered large oil fields. By the use of an advanced subsea pump technique it is possible to transport the oil from the well heads of samller oil reservoirs to the still existing oil production platforms by using subsea pipelines. Therefore it will be possible to explore new oil fields with the hardware of todays offshore oil production.

The reservoir fluid consists of crude oil, a remarkable amount of natural gas and also some solids. Using standard mechanical pumps will lead to bad efficiency because of the high gas fraction and the erasion inside of the pump due to the solids of the fluid. A pump unit is presented, which separates in a first stage the three phases oil, gas and solids. A single phase pump rises the oil to a high pressure level. Afterwards the oil depressurizes by forming a jet of high speed. Gas and solids, which have passed by the pump are remixed with the jet in a liquid jet pump. The mixture is recompressed by deceleration in the diffuser of the jet pump.

The test results have shown a good performance of this process. The experimental data were used to verify an analytical model of a full scale offshore plant.

Up to a void fraction of 50 % the system operates with sufficient efficiency. By separating the solids, erasion of the mechanical pump is prohibited, leading to low maintenance costs. Considering the extraordinary high service costs offshore, this is an important feature of a pump unit.

If the void fraction exceeds 50 %, an additional compressor for the gas phase is recommended.

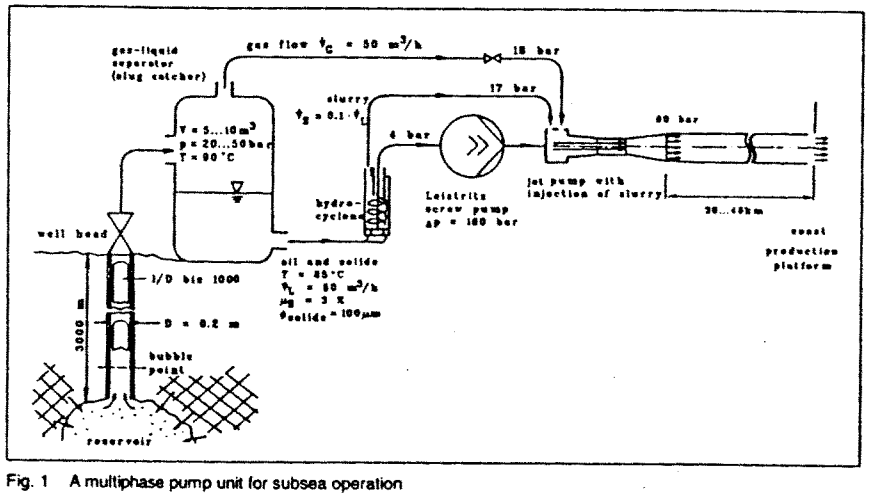

Fig. 1 A multiphase pump unit for subsea operation

1 Description of process

A study of the BP Exploration Co. Ltd. [1] shows, that the most unexplored but economically interesting oil reservoirs are situated within a maximum distance of 30 km away from existing oil production platforms. These new oilfields could be exploited by the use of still existing production and transportation equipment, if economically techniques for subsea pipeline transport of the crude oil were available. Due to the extraordinary high maintenance costs of offshore systems, new transportation technologies must operate without any need of service.

If one uses e.g. a one stage screw pump, the efficiency decreases with increasing void fraction. In addition the solids in the well head fluid, which have a fraction in the order of 2 % or 3 % cause erasion in the small sealing gaps of the machine, which will also lead to a loss in efficiency and short service intervals.

Figure 1 shows a subsea pump station, where the solids together with the gas are separated from the liquid.

Pressure shocks, caused by slug flow are damped by the use of a slug catcher. This device is also used as gas-liquid separator. Down stream of the slug catcher a hydro cyclone separates the solids in a slurry stream from the liquid flow.

The pure liquid is now compressed in a screw pump and depressurizes in a nozzle. A liquid jet of high velocity, which drives a jet pump, leaves the nozzle. Within the liquid jet pump gas and slurry are remixed and recompressed to a high pressure level.

In contrast to a one stage three phase pump there are two additional components, a hydro cyclone and a jet pump, necessary. But both devices are very simple, without moveable parts and a very reliable performance. As a result of the single phase flow within the screw pump it shows a high efficiency.

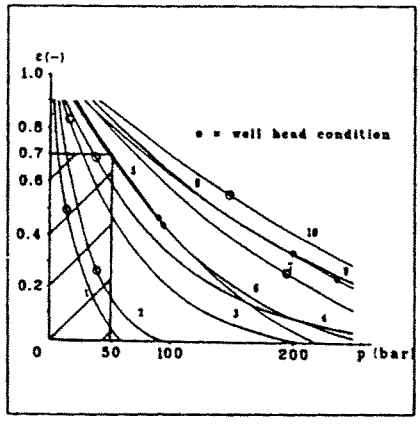

Fig. 2 Void fraction versus pressure for 10 typical reservoir fluids

2 Typical reservoir fluids

There are no general properties of crude oil. The density of different oil types vary as well as the viscosity. Furthermore the well head data like pressure, temperature and gas-oil-ratio and the extent of contamination differ within a wide range.

Properties of reservoir fluids, gained by measurements and derivated constitution laws were discussed by the authors of the papers [2] up to [9].

By plotting the void fraction ε versus the pressure p figure 2 shows the range of well known oil reservoirs. A decrease in pressure can lead to strong increase of the void fraction. The curves in Figure 2 show also the condition at the well head, marked by circles. On the right side the curves represent the oil condition inside the riser. At the left side the fluid conditions down stream of the well head within a pipeline or pump unit are shown.

*Dipl.-Ing. Th. Herpel, University of the Armed Forces, Munic; Dr. Ing. S. Muschelknautz, Linde AG, Höllriegelskreuth; o. Prof. Dr. Ing. F. Mayinger, Technical University of Munic, Munic/Germany.

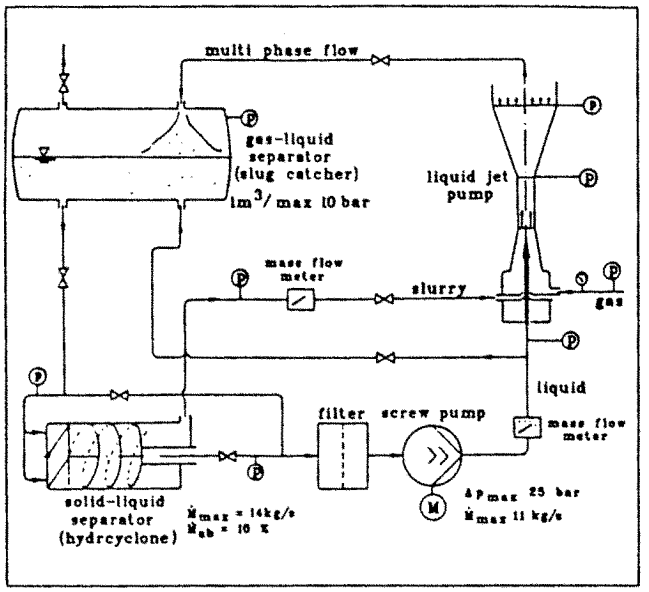

Fig. 3 Test facility

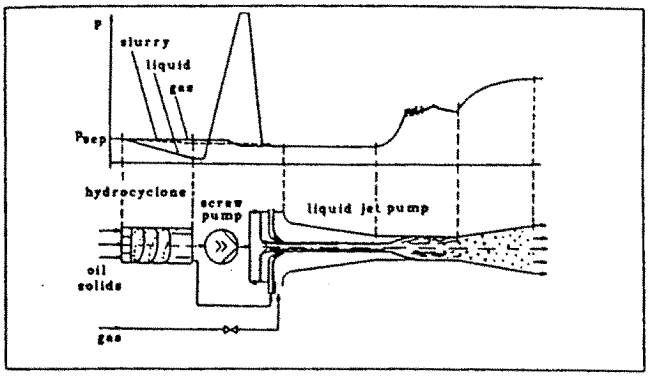

Fig. 4 Pressure course along the center line of the jet pump

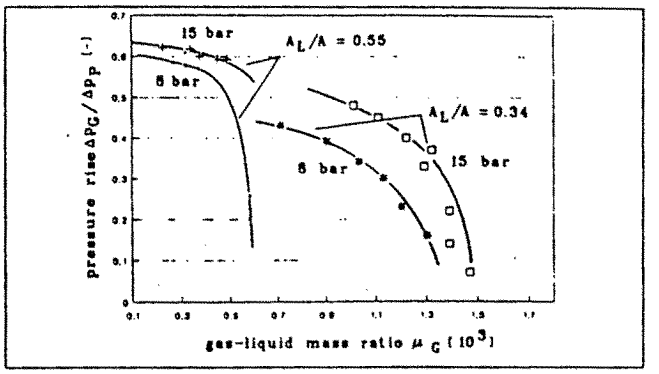

Fig. 5 Pressure rise across the jet pump for water air mixture, varied area ratio A_L/A and pressure differences of the screw pump of 8 bar and 15 bar

Multiphase pumps will be only established at oil reservoirs of low pressure levels, which do not allow a natural flow from the well head to the next production platform. Therefore fluids with well head pressures below 50 bar were only taken into account. A void fraction of up to 70 % should be handled by the pump unit. These assumptions lead to a operation range, which is marked also in Figure 2.

3 Test facility

All components of a real offshore pump unit were used at the test facility, represented in Figure 3.

Water was used as a test liquid as well as water-glycerin-mixtures of increased viscosity.

The gas phase of a reservoir fluid was simulated by air from the atmosphere. The pressure vessel of 1 m^3 content simulates the slug catcher.

The liquid leaves the vessel at the bottom to the liquid-solid separator, which splits the flow in two streams, a main stream with pure liquid and a slurry stream of liquid, contaminated with solids. A hydro cyclone, especially developed for oil-solid separation by the Institute for Mechanical Processing Engineering of the University of Stuttgart, was used as liquid-solid separator.

After passing a filter, the main stream flows to the screw pump, which can handle up to 40 m^3 liquid per hour, while the maximum pressure difference is about 25 bar. The high pressure fluid forms a high speed liquid jet for the liquid jet pump, which is capable for the suction of the slurry from the hydro cyclone as well as air from the atmosphere. It is also possible to feed the jet pump by air of a pressure level of up to 3 bar, leading to higher gas densities. The liquid, gas and slurry streams are remixed within the jet pump.

Down stream of the jet pump a throttle valve is used to simulate the pressure drop of the pipeline, which is connected with the pump station of a full scale offshore plant.

4 Liquid jet pump

4.1 General

The overall design of the liquid jet pump as well as its internal pressure are shown in Figure 4. Within the nozzle the liquid is accelerated, forming a liquid jet of small diameter but high velocity. Down stream of the nozzle the jet enters the suction chamber, where gas is entrained by viscous forces on the surface of the jet. The gas is forced to enter the mixing tube. In a sudden break up of the jet, called a mixing shock, gas and liquid are mixed, which is combined with a pressure rise due to sudden deceleration. Within the mixing shock the pressure distribution is unsteady.

Down stream of the mixing shock the gas-liquid-flow is still on high velocity and therefore has a high momentum. A diffuser, connected to the mixing chamber, reduces the flow velocity by rising the static pressure. Basic studies about jet pumps where done by Cunningham [11] and Dopkin [12].

4.2 Intake geometry and area ratio

The liquid jet pump was designed with a cylindrical mixing tube of 15 mm inner diameter in a first version. It was possible to change the lenght of the mixing tube. All tests were done with a diffuser of 270 mm lenght and an angle of 8 degree. The most important results of the tests are reported below. More detailed information can be found in [13].

The area ratio A_L/A is defined as the cross section of the liquid jet A_L divided by the cross section of the mixing tube A. Using a nozzle of 11 mm outlet diameter this ratio was $A_L/A = 0.55$. Figure 5 shows the ratio of measured pressure rise Δp_G of the jet pump to the pressure rise of the pump Δp_P, which is plotted against the gas-liquid ratio $\mu_G = M_G/M_L$. The results for 8 bar and 15 bar pressure difference of the screw pump are shown in Figure 5. Up to $\mu_G = 0.7 \cdot 10^{-3}$ the pressure ratio $\Delta p_G/\Delta p_P$ is about $0.6 \cdot 10^{-3}$. Within the jet pump there is a pressure rise of 60 % of the pressure difference of the pump. Exceeding the gas-liquid mass ratio over $\mu_G = 0.6 \cdot 10^{-3}$ leads to a decreasing pressure ratio.

Generally higher gas rates can be achieved by the use of greater intake areas for the air at the entrance of the mixing tube. The corresponding test results are also plotted in Figure 5 for an area ratio of $A_L/A = 0.34$. Remarkable higher gas-liquid ratios of $\mu_G = 1.5 \cdot 10^{-3}$ were measured at $\Delta p_G/\Delta p_P = 0.4$.

A conical air intake led to a further increased intake area. The mixing shock is still located in the cylindrical part of the tube, where the area ratio is still the same. There was an orifice used as a nozzle. Although there was a slight decrease in pressure ratio, the conical intake allowed to have about 10 % higher gas-liquid ratios, compared to the cylindrical intake, see Figure 6. To reduce all pressure losses at the air intake to a minimum, a testrun was done without having an air intake chamber. The liquid jet passed free atmosphere before entering the mixing tube. But no significant increase of the gas rate could be achieved.

4.3 Variation of the gas density

In order to investigate the jet pump performance with higher gas densities at the entran-

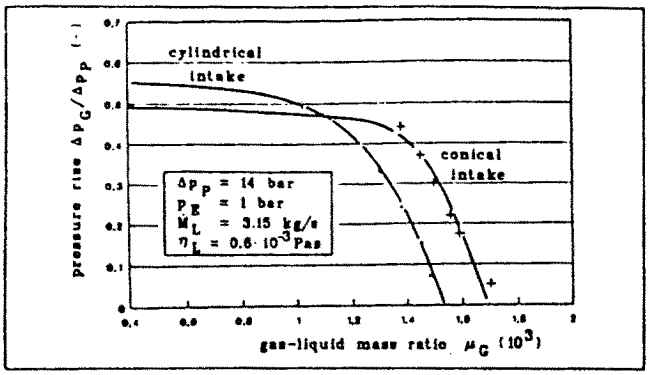

Fig. 6 Experimental data for cylindrical and conical air intake

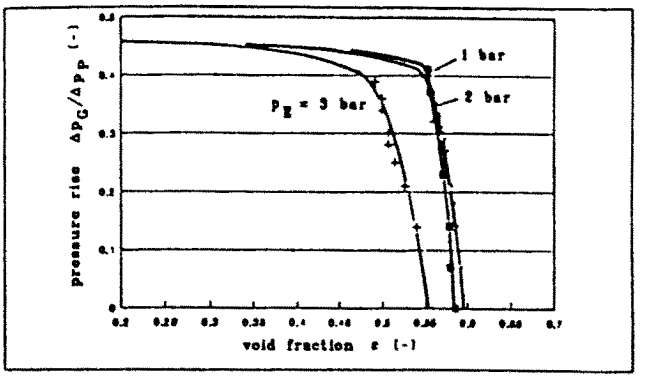

Fig. 7 Pressure rise and void fraction for the jet pump at different static pressure of gas and different gas densities

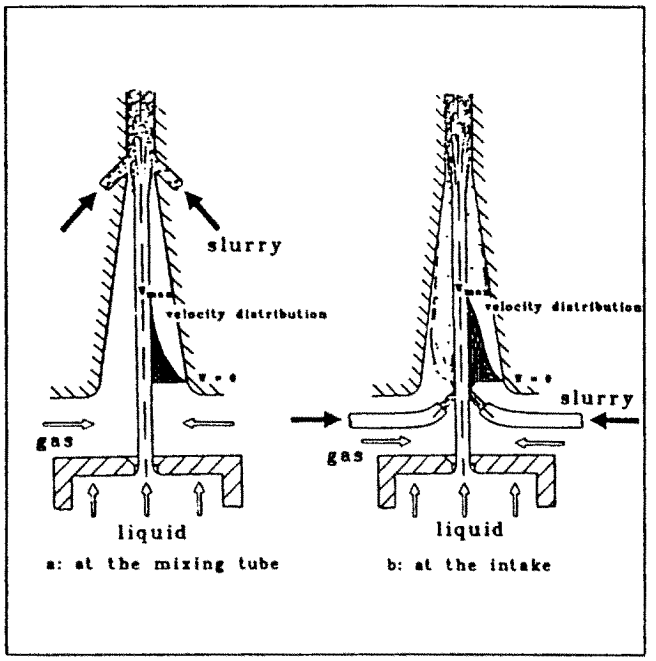

Fig. 8 Different arrangements for slurry injection

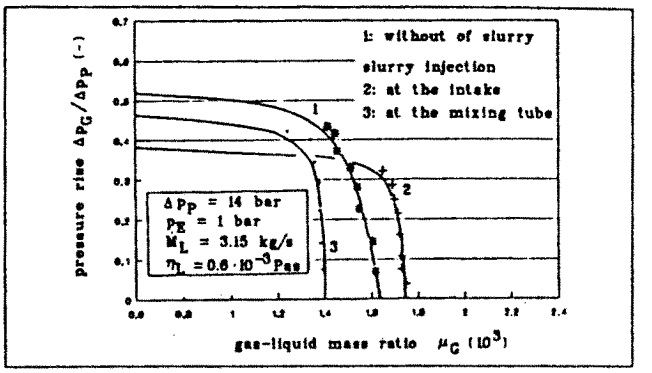

Fig. 9 Pressure rise against gas-liquid mass ratio for different slurry injection arrangements

ce of the jet pump, air on a pressure level of 2 bar and 3 bar was fed to the jet pump. For having equal jet velocities, the pressure difference between pump outlet and static pressure of the air intake were the same as on low density tests. Due to higher gas densities significant higher gas mass flow rates were possible. But the void fraction ε, as plotted in Figure 7, decreases slightly at higher gas pressure levels. This is a result of the constant momentum of the jet which has to accelerate an increased mass of gas.

4.4 Slurry injection

The oil-solid slurry from the solid separator has to be added to the main stream again after the pump at a section of low pressure. This is between the nozzle and the mixing shock of the jet pump.

Figure 8 a shows the design of a jet pump with slurry injection just before the mixing shock. In this section of the tube the jet velocity has already decreased. A small pressure difference of about 1 bar based on the gas pressure at the air intake is sufficient for the slurry injection. No inefficient acceleration up to an extreme high jet velocity, like in the case of injection just after the nozzle, and subsequent deceleration of the slurry stream is necessary. Curve 3 of Figure 9 shows test results for this option. While the pressure ratio achieved is only slightly below that of the jet pump without slurry injection, the gas-liquid mass ratio decreases remarkable.

Another arrangement of the slurry injection, shown in Figure 8 b, was also tested. There were two slurry jets added to the main liquid jet of the jet pump at the air intake section. Due to the differences in velocity of liquid and slurry, the surface of the liquid jet was scattered and a lot of droplets, which were spread around the jet, could be observed. These droplets help to accelerate gas and therefore to increase the gas rate, see curve 3 in Figure 9. On the other hand the overall pressure rise of the liquid jet pump decreases, compared to a jet pump without slurry injection.

4.5 Increased liquid viscosity and proper mixing tube design

For the investigation of the influence of an increased liquid viscosity a mixture of glycerine and water was used at the test facility. This test fluid had at test conditions a viscosity of $8 \cdot 10^{-3}$ Pa·s, which is 12 times the viscosity of pure water, as used for the first tests. A strong influence of liquid viscosity on the mixing behaviour of the jet could be observed. Because of the higher viscous forces, which are needed for the jet break up, the jet is able to travel a longer way along the tube before breaking up in the mixing shock. The mixing tube had to be redesigned to prevent the mixing shock from being located in the diffuser. It could be also observed, that due to the more viscous liquid there were less droplets scattered from the surface of the jet at the gas intake, which help to accelerate gas in this section. This leads to lower gas rates, which were about 20 % below corresponding gas-liquid ratios of pure water tests. Furthermore a more viscous liquid induces higher pressure losses by increased friction in the two-phase section of the mixing tube. This leads to lower total pressure rises for the jet pump. Therefore it is important to have the mixing shock, which is follwed by a two-phase flow in contact with the inner wall of the tube, located at the end of the mixing tube. The pressure rise of the system versus the gas-liquid mass ratio is plotted in Figure 10 for different dimensions of the tube. High gas rates combined with common pressure ratios could be measured for a tube with a lenght to diameter ratio of L/D = 32. A pressure ratio of $\Delta p_G/\Delta p_P = 0.28$ can be achieved with a gas-liquid ratio of $\mu_G = 1.1 \cdot 10^{-1}$. The corresponding void fraction is $\varepsilon = 48$ %.

5 Mathematical model

Within the jet pump gas is accelerated by viscous forces at the surface of the liquid jet and by droplets, separated from the jet. Due to the mixing shock, there is a sudden pressure rise. This unsteady flow cannot be des-

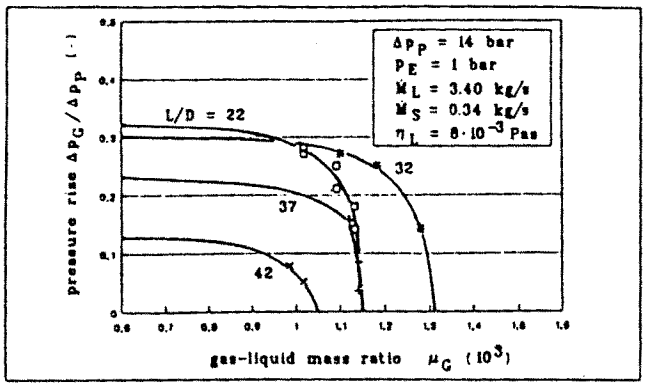

Fig. 10 Pressure rise against gas-liquid mass ratio for liquid with increased viscosity and slurry injection

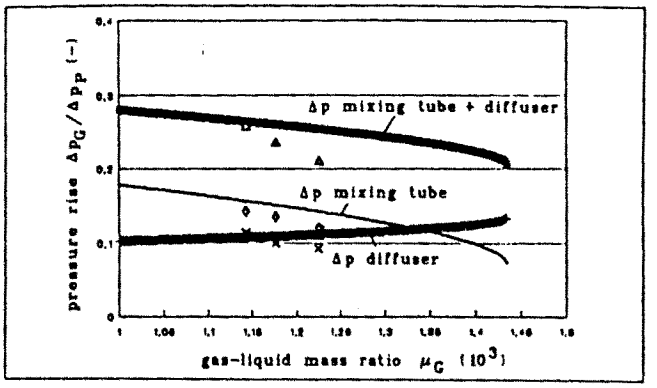

Fig. 11 Comparison of experimental and theoretical data for a jet pump with slurry injection and a liquid viscosity of $\eta = 8 \cdot 10^{-3}$ Pa·s

cribed in detail. Therefore the mathematical model is based on the overall momentum equation.

Equation (1) describes the pressure at the exit of the mixing tube, p_M, depending on the inlet pressure p_E, the pressure of the pump p_P^*, ρ^* and $\rho_{G,M}$, the momentum coefficients β and geometrical data:

$$p_M = p_E + \rho^* \cdot 2 \cdot \left(p_P^* - p_E\right) \cdot \left(\frac{A^*}{A}\right)^2 \cdot \left[\beta^* \cdot \frac{1}{\rho^*} \cdot \frac{\frac{1}{A^*}}{\frac{A}{A}} + \mu^{*2} \cdot \frac{1}{\rho_{G,M}(p_M)} \cdot \frac{\frac{1}{A_G}}{\frac{A}{A}} - \beta_M \left(\mu^* + 1\right) \cdot \left(\frac{1}{\rho^*} + \frac{\mu^*}{\rho_{G,M}(p_M)}\right)\right] + \Delta p_{2ph,Chisholm} \quad (1)$$

The density of gas at the exit of the mixing tube $\rho_{G,M}$ is a function of the pressure p_M. Therefore equation (1) has to be solved by transformation to a quadratic form or by successive approximation. [13] gives the derivation of equation (1) in detail.

The calculation of the pressure rise of the diffuser is based on homogeneous two phase flow at the exit of the mixing tube. By the use of a diffuser efficiency η_{diff} and the mean density of the two phase flow ρ_M the pressure rise of the diffuser Δp_{diff} is represented by equation (2):

$$\Delta p_{diff} = \eta_{diff} \cdot \frac{\rho_M}{2} \cdot w_M^2 \quad (2)$$

The efficiency η_{diff} was about 80 % for the test diffuser at two phase mode. Using the results of equation (1), it is also possible to represent the pressure recovery of the diffuser by equation (3):

$$\Delta p_{diff} = \eta_{diff} \cdot \left(p_P^* - p_E\right) \cdot \rho^* \cdot \left(\frac{A^*}{A}\right)^2 \cdot \left(1 + \mu^*\right) \cdot \left(\frac{1}{\rho^*} + \frac{\mu^*}{\rho_{G,M}(p_M)}\right) \quad (3)$$

The total pressure rise of the jet pump Δp_G is the sum of the pressure differences of the mixing tube and the diffuser. It is unified with the pressure differences of the screw pump Δp_P:

$$\frac{\Delta p_G}{\Delta p_P} = \frac{p_M - p_E + \Delta p_{diff}}{\Delta p_P} \quad (4)$$

The presented analytical model of the jet pump was verified with the experimental data. Input data were the design data, the properties of the fluids and the gas rate. Calculated data were the pressure differences of the mixing tube, the diffuser and the total pressure difference of the jet pump, plotted at Figure 11. Slurry injection and high viscosity fluid were used in this test and also in the calculations. Calculations as well as test results show a decrease in pressure rise of the jet pump with increased gas rates.

With respect to the velocity profile at the exit of the mixing tube, which is of great influence on the correlated momentum, the momentum coefficient β was used in equation (1). Measurements of the velocity profile led to momentum coefficients of $\beta = 1.08 \ldots 1.1$. Only at the exit of very long mixing tubes smaller momentum coefficients about $\beta = 1.02$ were detected. For the first quarter of the calculated pressure curves, shown in Figure 11, no measurement data are available, because the jet pump does not work in a steady state mode at low gas rates. As the small slope of the curves show, a very small change in pressure leads to great changes of the gas rate.

For gas-liquid ratios of more than $\mu_G = 1.15 \cdot 10^{-3}$ and above the tested jet pump had smaller pressure rises than predicted by the model. At this gas rates the flow within the jet pump does no longer meet the assumptions of the calculation. Increasing gas rates lead to a more and more misplaced mixing shock, which is located in the diffuser at worst case conditions.

As the tests have shown, the jet pump has a relatively small range of operation, where a maximum pressure rise is combined with satisfactory gas rates, like the measurement data at $\mu_G = 1.15 \cdot 10^{-3}$ in Figure 11. This design point of the jet pump is well represented by the analytical model.

The length of the mixing tube was used for the calculation of the two phase loss within the tube. But there is no way to calculate the location of the mixing shock, which has a direct influence on the behaviour of the jet pump and is strong depending on the viscosity of the fluid. A guide for further design of mixing tubes could be the experiences of the tests, which are summarized in Table 1.

6 Range of operation

A theoretical model was presented before, which predicts the pressure difference for the test jet pump at its design point. While the separation characteristic of the solid-liquid separator was well known from detailed work on this device, it was possible to describe its behaviour with a simple mass balance. The pressure losses in the piping arrangement of the pump unit can be described by common calculations. Both was done in order to complete the simplified model which was now capable to prescribe the behaviour of a full scale pump unit. For details see [13].

Reservoir fluids are contaminated with solids of about 3 % of the whole mass flow rate. Within the solid-liquid separator the incoming flow is splitted to a slurry stream of 10 % and a liquid stream of 90 %. A model fluid was created with properties which represent the variety of possible fluids:

Density of oil, kg/m³ $\rho_{oil} = 865$
Viscosity of oil, Pa·s $\eta_{oil} = 0.01635 - 0.000175 \cdot p$
Density of gas, kg/m³ $\rho_{gas} = 0.998 \cdot p$
Viscosity of gas, Pa·s $\eta_{gas} = 1.392 \cdot 10^{-5} + 2.28 \cdot 10^{-7} \cdot p$

(p – pressure, bar,
all data for model oil at 85 °C)

A pressure difference of the screw pump of $\Delta p_P = 160$ bar was used for the calculations. This will lead to high velocities within the mixing tube. The chose of a relative short mixing tube with L/D = 20 helps to reduce the pressure loss of the tube.

There are two essential input data for an offshore plant: The void fraction ε_{SEP} and the pressure of the fluid p_{SEP} at the entrance of the slug catcher. Those parameters were varied on a wide range for the prediction of the behaviour of a full scale plant, as shown by the bottom axis in Figure 12. The calculated pressure rise of the plant, unified with the pressure difference of the screw pump, is represented by the vertical axe of the graph.

As known from the experimental data the liquid jet pump has a small range of operation with high gas rates and proper outlet pressure. Therefore it is not useful to operate the jet

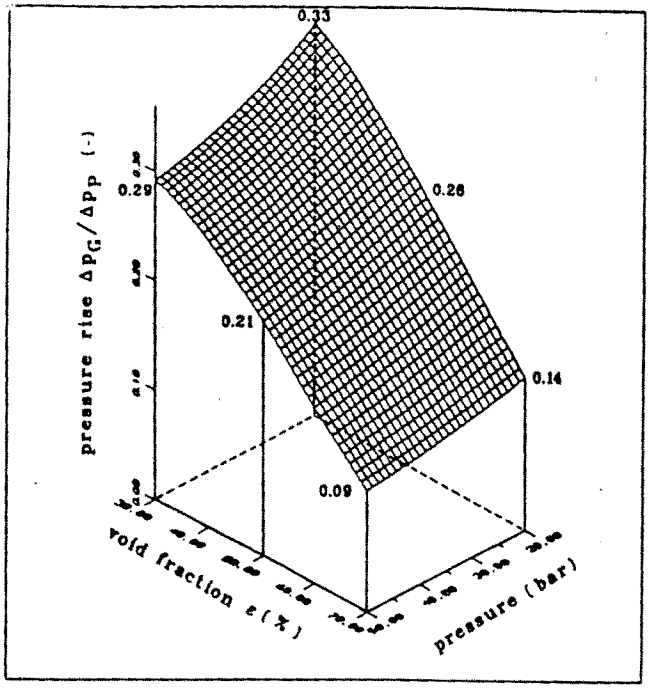

Fig. 12 Calculated pressure rise of a full scale multiphase pump unit

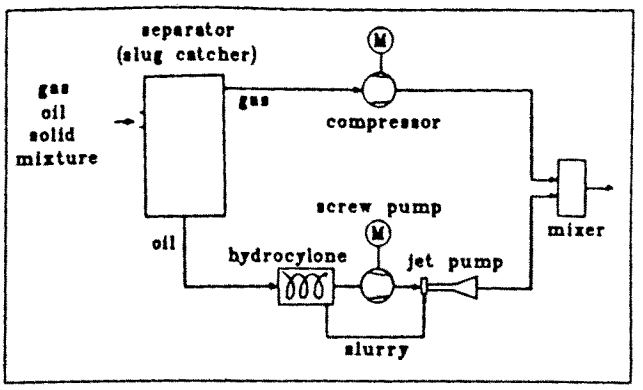

Fig. 13 Process of a multiphase pump unit based on I liquid-liquid jet pump and an additional compressor for fluids of extreme high gas rates

pump far from its design point. Obviously figure 12 represents a wide range of input data, which could be handled by different pump units especially designed for each point but not the operation range of one single plant.

As known from the tests there is a downward tendency of the pressure rise with increasing gas rate and input pressure. For instance at an entrance pressure of 20 bar and a void fraction of ε_{SEP} = 50 % the unit will have a unified pressure rise of $\Delta p_G/\Delta p_P$ = 0.25. I.e. the pressure rise of the three phase flow is 25 % of the pressure difference of the screw pump of 160 bar, working on pure oil.

Table 1 **Test range**

viscosity of liquid, 10^{-3} Pa·s	area ratio	ratio of length and diameter of the mixing tube L/D
0.65*	0.28 - 0.40	22
0.65*	0.40 - 0.60	18
8.0*	0.30 - 0.40	32

*for test temperatures of 40 °C

Table 2 **Power consumption**

	jet pump process	multiphase screw pump
Δp_G, bar	40	40
Δp_{pump}, bar	160	40
$\dot{V}_{pump}$, m^3/h	45	100
η_{pump}	0.75	0.4*
P_{pump}, kW	265	220*

*efficiency losses caused by solids within the screw pump are not considered

This will result in a total pressure rise of 40 bar for the multi phase fluid. Smaller gas rates lead to increased pressure rises up to 33 %.

The minimum unified pressure rise of $\Delta p_G/\Delta p_P$ = 0.09 occurs on flow conditions of ε_{SEP} = 70 % and p_{SEP} = 50 bar. It seems not useful to have a pump unit working on those input conditions.

7 Process variations

For the comparison of different processes, the power requirement of the pump P is one important parameter. With the pressure difference of a pump Δp_P, the fluid rate $\dot{V}P$ and the pump efficiency η_P its power need is given by equation (5):

$$P = \frac{\Delta p_p \cdot \dot{V}_p}{\eta_p} \qquad (5)$$

For normal operation of the liquid jet pump a considerable Δp_P is required. But the fluid rate $\dot{V}P$ is low, because the liquid is compressed within the screw pump only. For instance at ε_{SEP} = 50 % $\dot{V}P$ is only 45 % of the total flow rate.

Some simplifying assumptions made it possible to calculate the power consumption of the here presented plant and also that of a one stage multiphase screw pump, working on oil, gas and solids. The results are presented in Table 2, based on a void fraction of 50 % and an input pressure of 20 bar. Equations for calculation of the power consumption of the one stage multiphase pump and corresponding efficiencies were taken from [15].

According to Table 2 the power consumption of the jet pump process is not significantly higher than that of a multiphase pump. Due to erasion a screw pump, operating on solid contaminated fluids, suffers from efficiency losses. Those effects could not have been considered for the figures of Table 2.

In addition economic aspects like increased maintenance effort and the increased risk of a total failure of the pump have to be taken into account.

If reservoir fluids of high gas rates have to be pumped, a compressor for the gas phase is recommended, see Figure 13. The liquid pump will still be protected from solids by the solid-liquid separator. The jet pump will be of the liquid-liquid type, which is used to pump the slurry to the output pressure. Compressed gas and oil with solids are remixed for the common transport on a pipeline.

Nomenclature

p	pressure
Δp	pressure difference
P	power consumption for the pump
A	cross section area
w	velocity
$\dot{M}$	mass flow rate
$\dot{V}$	volume flow rate
ρ	density
ε	void fraction
μ_G	gas-liquid mass ratio MG/ML
μ_S	solid-liquid mass ratio MS/ML
η	dynamic viscosity
η_{diff}	diffuser efficiency
η_P	pump efficiency
β	momentum coefficient

Indices

G	gas
S	slurry
L	liquid
SEP	separator
E	entrance of mixing tube
M	mixing tube exit
*	after premixing of liquid and slurry
2ph.Chsh.	two phase pressure loss from [14]

The here presented research activities were sponsored by the German Ministry of Research and Technology with the Number 0326676G. The authors are responsible for the content.

References

[1] FRANCIS, A. K.; LEGGATE, J. S.; STEPHENSON, G. W.: Developments in the Application of Multiphase Systems to Oil Production Schemes. Chem. Eng. Res. Des., Vol. 66, July 1988, S. 300 - 312.

[2] MAYER-GÜRR, A.: Petroleum Engineering. Ferdinand Enke Publishers, Stuttgart 1976.

[3] BRECHT, C.; GRAZKOWSKI, H.-W.: Gewinnung und Transport von Erdöl und Erdgas. Carl Hanser Verlag, München 1982.

[4] SZILAS, A. P.: Production and Transport of Oil and

Gas. Elsevier Scientific Publishing Company, Amsterdam 1975.

[5] MOSES, P. L.: Engineering Applications of Phase Behavoir of Crude Oil and Condensate Systems. Journal of Petroleum Technology, July 1986, S. 715 - 723.

[6] AHRABI, F.; ASHCROFT, S. J.; SHEARN, R. B.: High Pressure Volumetric Phase Composition and Viscosity Data for a North Sea Crude Oil and NGL. Chem. Eng. Res. Des., 65, January 1987, S. 63 - 73.

[7] FIROOZABADI, A.: Reservoir-Fluid Phase Behavior and Volumetric Prediction with Equations of State. JPT, April 1988, S. 397 - 406.

[8] COATS, K. H.: Simulation of Gas Condensate Reservoir Performance. JPT, October 1985, S. 1879 - 1886.

[9] VAROTSIS, N. et al.: Phase Behavior of Systems Comprising North Sea Reservoir-Fluids and Injection Gases. JPT, November 1986, S. 1221 - 1233.

[10] WURTZ, R.; SCHLAG, P.; MUSCHELKNAUTZ, E.: Feststoffseparation von Erdöl mit Hilfe eines Zyklonabschneiders, Abschlußbericht, Institut für Mechanische Verfahrenstechnik, Universität Stuttgart, 1990.

[11] CUNNINGHAM, R. G.: Gas Compression with the Liquid Jet Pump. Trans. A.S.M.E. Ser. I.J. Fluids Engineering, 96, September 1974, S. 203 - 214.

[12] DOPKIN, R. J.; CUNNINGHAM, R. G.: Jet Break-Up and Mixing Throat Lenght of the Liquid Jet Gas Pump. Trans. A.S.M.E. Ser. I.J. Fluids Engineering, 96, September 1974, S. 216 - 226.

[13] HERPEL, Th.; MUSCHELKNAUTZ, S.; MAYINGER, F.: Abscheidung und Wiedereinmischung von Feststoff bei Unterwasserförderung von Öl zum Schutz der Förderpumpe und Feinabscheidung von Öl aus Wasser, Abschlußbericht, Lehrstuhl A für Thermodynamik, Technische Universität München, 1990.

[14] CHISHOLM, D.: Int. J. Heat and Mass Transfer 16, pp. 347ff., 1973.

[15] KARGE, V.: Schraubenspindelpumpen zur Förderung von Multiphasengemischen. Pumpen, Vakuumpumpen, Kompressoren, 1988, S. 14 - 20.

Flow Behaviour of Saudi Heavy Crude Oil Emulsions under Turbulent Conditions

*By A. E. OMAR, S. E. M. DESOUKY and B. K. ABDALLA**

Abstract

Rheological characteristics of Saudi heavy crude oil emulsions were measured with a Haak Rotovisco Model (RV-11) rotational viscometer at temperatures ranging from 0.0 to 40.0 °C in steps of 10.0 °C. The oil-in-water emulsion employed had oil concentrations of 10.0, 30.0, 50.0, 70.0 and 90.0 % by volume, with emulsifying agent concentrations of 0.25, 0.50, 0.75, 1.0, and 1.25 % by volume for each oil concentration.

A new rheological model which relates the shear stress with shear rate, temperature, oil and emulsifying agent concentration was developed. The Metzner and Reed parameters n' and k', required for pipeline design were incorporated as functions of the model parameters. The effects of temperature and concentrations of oil as well as emulsifying agent on pipeline design under turbulent conditions were studied. The results show that the pressure required to pump Saudi heavy crude oil emulsions is less than that required to pump the heavy crude oil.

Introduction

An extensive study of the rheological behaviour of crude oil emulsions is indispensable for evaluation of energy consumption, operational safety and cost effectiveness of transportation of such emulsions through a pipeline (Wyslouzil, et al., 1987). A change in the rheological characteristics of crude oil emulsions, due to thermal and shear history of oil concentration, strongly affects the pipeline design. Although several studies have reported significant effects of temperature and concentrations of emulsifying agents and oils on the rheological behaviour of crude oil emulsions, no agreement has emerged on a generalized correlation between such effects on pipeline design (Marsden and Rose, 1971; Marsden, 1971; Marsden and Raghavan, 1973; Zakin, et al., 1979; Yildirim, et. al., 1988).

In this article the effects of temperature, oil and emulsifying agent concentrations on the rheological behaviour of Saudi heavy crude oil emulsions (SHCOE) were studied experimentally and described mathematically. A new rheological model involving the effects of the temperature, oil and emulsifying agent concentrations was developed. Two relations were also developed to relate the Metzner and Reed (1955) parameters (n and k) to those of the rheological model developed. These two relations and the Dodge and Metzner (1959) equations were used to study the effect of temperature, oil and emulsifying agent concentrations on the pressure required to pump such emulsions in AL-Jubial-Yanbu pipeline (Al-Fariss and Desouky, 1990).

*Adnan E. Omar, Saad E. M. Desouky and Babiker K. Abdalla, Petroleum Engineering Dept., King Saud University, Riyadh, Saudi Arabia.

Experimental work

The rheological characteristics of SHCOE were measured with a Haak Rotovisco Model (RV-11) rotational viscometer at temperatures of 0.0, 10.0, 20.0, 30.0 and 40.0 °C. The oil concentrations employed were 10.0, 30.0, 50.0, 70.0 and 90.0 % by volume. The emulsifying agent used was Triton-X100 in concentrations of 0.25, 0.5, 0.75, 1.0 and 1.25 % by volume for each oil concentration. The salinity of the brine used to form the emulsion was 15.0 % NaCl (by weight) which is the average salinity of the Saudi formation water.

In order to duplicate the time in flow equipment in a typical experiment, the sample of the prepared emulsion to be tested was placed in the viscometer and stirred at the specified test temperature for four hours before the measurements were made. The rotational speed was then increased and the corresponding shear stress and shear rate were recorded.

Results and discussion

Some of the rheological characteristics measured are given in Fig. 1. The data obtained were used to develop the new rheological model employing the pseudo-analysis technique (Levenlspiel, 1970). The model is as follows:

$$\tau = \left[\frac{1.304\,(EAC)^{0.0274}\,(OC)^{0.36}}{T^{0.0347}} \right] \dot{\gamma}^{0.663} \qquad (1)$$

where

τ – shear stress, Pa

$\dot{\gamma}$ – shear rate, s

T – temperature, °C

OC – oil concentration, % by volume